

STUDY ON TEMPERATURE DEPENDENT ELECTRICAL PROPERTIES OF COBALT-ZINC NANOFERRITES

Htet Naing Lwin¹, Thinn Thinn Tun², Cho Cho Aung³ & Win Kyaw⁴

Abstract

Spinel ferrites have been studied extensively because they play a vital role in the technological applications. In the present work, Cobalt-Zinc nanoferrites, $\text{Co}_{1-x}\text{Zn}_x\text{Fe}_2\text{O}_4$ (where $x = 0.0, 0.1, 0.2$ and 0.3) have been prepared by auto-combustion method. Structural and microstructural properties of the samples were characterized by X-ray diffraction (XRD) and Scanning Electron Microscope (SEM) to investigate the single phase nanosized ferrites and morphological features of grain shape, grain size and homogeneity. Variation of the dc electrical resistivities of the Cobalt ferrites with the different concentrations of Zinc was observed by a simple two probe method. Temperature dependent electrical conductivities of the samples were investigated in the temperature range of 303 K – 773 K. The activation energies (E_a) of the samples were evaluated by using the slopes of $\ln\sigma - 1000/T$ relationships.

Keywords: Cobalt-Zinc nanoferrites, auto-combustion method, XRD, SEM, electrical conductivities

Introduction

Spinel ferrites have been studied extensively because they play a vital role in the technological applications. Ferrites have good electric properties and a large number of applications from microwave to radio frequency [Ahmad, (2012)]. The dielectric properties of these ferrites are very sensitive to the method of preparation and sintering condition. Therefore, the selection of an appropriate process is the key to obtain high quality ferrites [Pathan, (2010)].

¹ PhD Candidate, Assistant Lecturer, Department of Physics, University of Yangon

² Dr, Assistant Lecturer, Department of Physics, Dagon University

³ Dr, Associate Professor, Department of Physics, University of Yangon

⁴ Dr, Associate Professor, Department of Physics, Sagaing University

The ability to prepare nanostructures with defined morphologies and sizes in large scale is an essential requirement for applications in nanomaterials [Harris, (2009); Iyer, (2009)]. As a result, extensive efforts have been devoted to develop synthetic capabilities to produce nanomaterials with tailored magnetic and electrical properties. The properties of nanomaterials are remarkably different from that of their bulk counterpart [Marial, (2013)]. The interest in ferrite nanoparticles is due to their important physical and chemical properties and potential for various technological applications such as high density magnetic storage, electronic and microwave devices, sensors, magnetically guided drug delivery etc [Rani, (2013)]. A large number of methods has been developed to prepare $\text{Co}_{1-x}\text{Zn}_x\text{Fe}_2\text{O}_4$ (CZFO) ferrite nanoparticles, such as the Co-precipitation, Auto-Combustion method, Sol-gel method, Solvothermal method, the standard solid-state reaction technique and the hydrothermal method. Further, the electrical and dielectric properties of cobalt-zinc nanoferrites were reported by many workers. In this work, the structural, microstructural and electrical properties of Co-Zn ferrite nanoparticles prepared by solution combustion method and characterized by XRD, SEM and electrical conductivity measurements are reported.

Experimental Details

Preparation of Zinc substituted Cobalt Ferrites

Zinc substituted Cobalt ferrites, $\text{Co}_{1-x}\text{Zn}_x\text{Fe}_2\text{O}_4$ (where $x = 0.0, 0.1, 0.2$ and 0.3) have been prepared by auto-combustion method. The chemical reagents used in this work were Zinc Nitrate Hexahydrate [$\text{Zn}(\text{NO}_3)_2 \cdot 6\text{H}_2\text{O}$], Cobalt (II) Nitrate Hexahydrate [$\text{Co}(\text{NO}_2)_2 \cdot 6\text{H}_2\text{O}$], and Ferric Nitrate Nonahydrate [$\text{Fe}(\text{NO}_3)_3 \cdot 9\text{H}_2\text{O}$]. Urea [$\text{CO}(\text{NH}_2)_2$] was used as a fuel. Sample preparation procedure of the $\text{Co}_{1-x}\text{Zn}_x\text{Fe}_2\text{O}_4$ is shown in Figure 1. Photographs of the preparation of the $\text{Co}_{1-x}\text{Zn}_x\text{Fe}_2\text{O}_4$ samples (e.g., $x = 0.1$), DELTA A SERIES Temperature Controller DTA-4896 and experimental setup of the sample preparation system are shown in Figures 2(a – n).

XRD, SEM and Electrical Properties Measurements

Structural analysis, lattice parameters calculation and crystallite size estimation of the samples were investigated by XRD method. XRD patterns were observed by RIGAKU MULTIFLEX X-ray Diffractometer using Ni-filter with CuK_α radiation, $\lambda = 1.54056 \text{ \AA}$. Microstructural properties of the samples were investigated by using JEOL JSM-5610LV SEM with the accelerating voltage of 15 kV, the beam current of 50 mA and 5500 times photo magnification. For the electrical properties measurement, the samples were made into pellets. The electrical resistances of the samples were observed in the temperature range of 303 K – 773 K by using FLUKE 45 Dual-display digital multi-meter. In this measurement, Autonics TCN4L – 24R Temperature Controller and K-type thermocouple were used as the temperature controller and temperature sensor. Photographs of the experimental setup of electrical conductivity measurement are shown in Figure 3(a) and (b) respectively. Thickness and area of each of the sample were 2.19 mm and $1.14 \times 10^{-4} \text{ m}^2$.

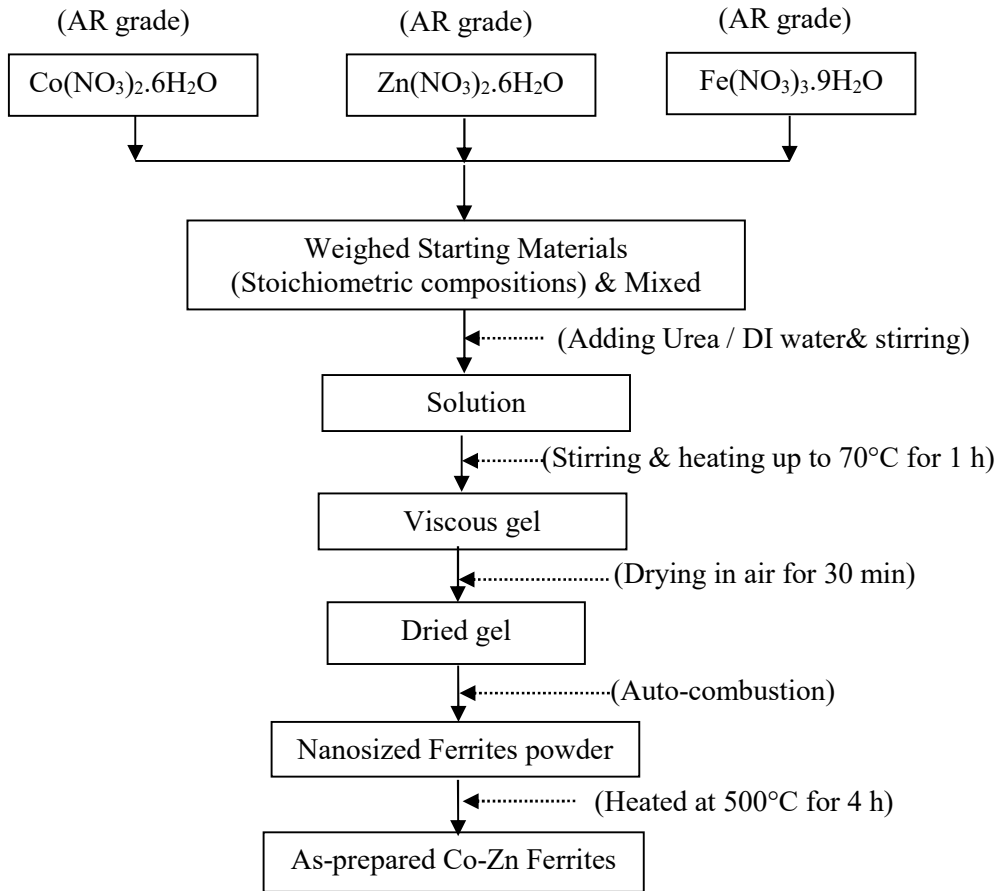


Figure 1. Flow-diagram of the preparation procedure of Co-Zn ferrite



Figure 2. Photographs of the starting materials of AR grade (a)Fe(NO₃)₃·9H₂O, (b) Zn(NO₃)₂·6H₂O, (c) CO(NH₂)₂ and (d) Co(NO₃)₂·6H₂O

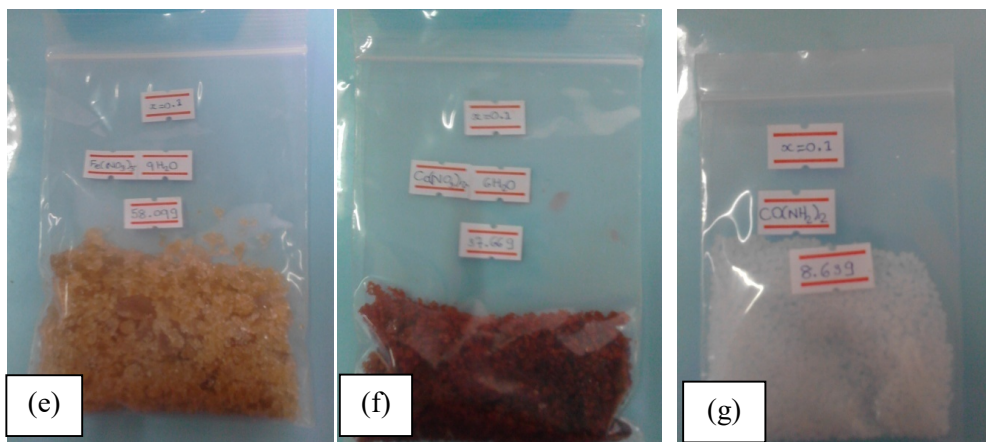


Figure 2. Photographs of the weighed starting materials of (e)Fe(NO₃)₃·9H₂O, (f) Co(NO₃)₂·6H₂O and (g)CO(NH₂)₂

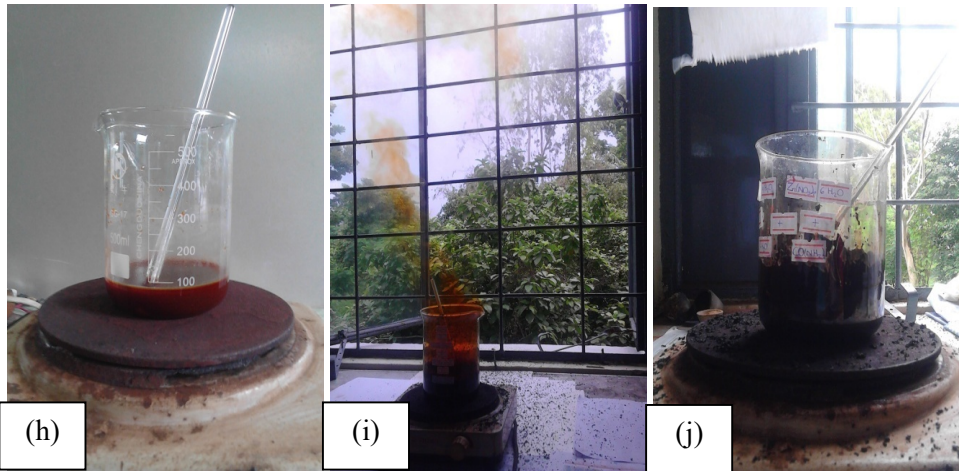


Figure 2. Photographs of the (h) mixed solutions of starting materials, (i) self-combustion occurring and (j) after self-combustion

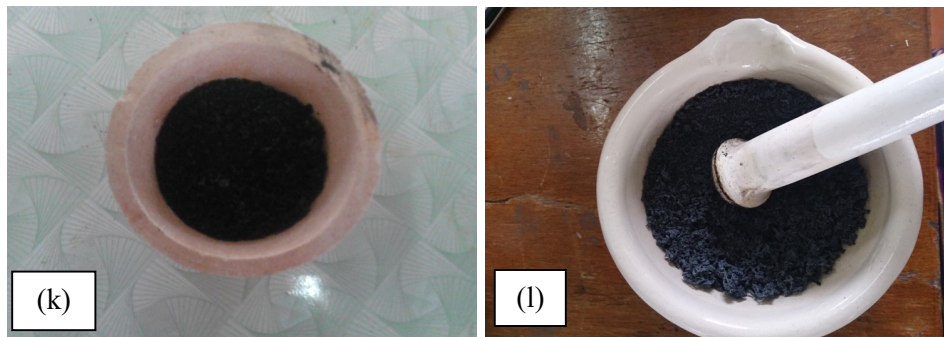


Figure 2. Photographs of the (k) combustion ferrite and (l) crushing of as-prepared ferrite

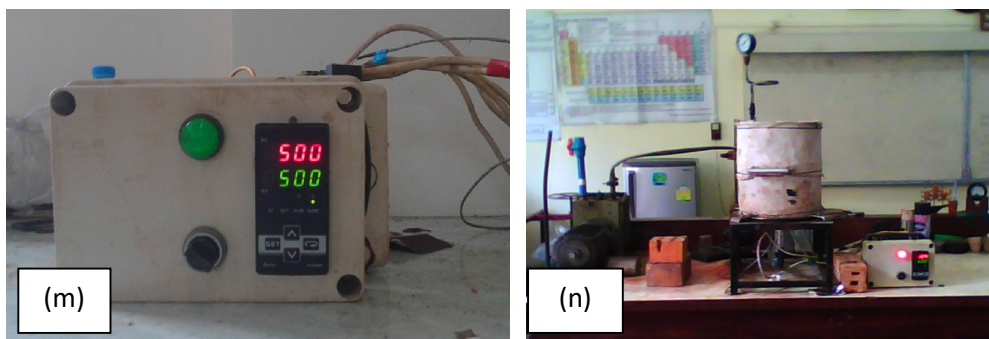


Figure 2. Photographs of the (m) DELTA A SERIES temperature controller DTA-4896 at 500°C and (n) experimental setup of sample preparation system

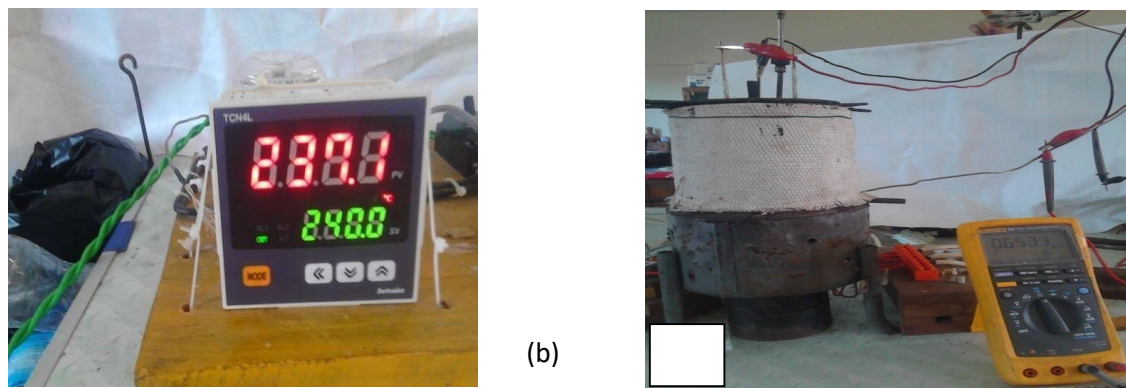


Figure3. Photographs of the (a) temperature controller Autonics TCN4L – 24R and (b) experimental setup of electrical conductivity measurement

Results and Discussion

XRD Study

Powder X-ray diffraction patterns of $\text{Co}_{1-x}\text{Zn}_x\text{Fe}_2\text{O}_4$, (where $x = 0.0, 0.1, 0.2$ and 0.3) samples are shown in Figure 4(a – d). The observed XRD lines were identified by using standard JCPDS data library files of

- (1) Cat. No. 03-0864> CoFe_2O_4 – Cobalt Iron Oxide for CoFe_2O_4 sample and
- (2) Cat. No. 89-7412> Franklinite – ZnFe_2O_4 and Cat. No. 03-0864> CoFe_2O_4 – Cobalt Iron Oxide for $\text{Co}_{0.9}\text{Zn}_{0.1}\text{Fe}_2\text{O}_4$, $\text{Co}_{0.8}\text{Zn}_{0.2}\text{Fe}_2\text{O}_4$ and $\text{Co}_{0.7}\text{Zn}_{0.3}\text{Fe}_2\text{O}_4$.

The entire samples under investigation shows the characteristics peaks of cubic crystalline ferrite material with the most intense peak (311). All the samples show good crystallization with well defined peaks. The observed XRD patterns exclude the presence of any undesirable secondary phase. The slight broadening of the XRD peaks indicates that the samples have nano-crystalline nature.

The lattice parameters were calculated by using crystal utility of the equation: $a = \frac{\lambda}{2 \sin \theta} \sqrt{h^2 + k^2 + l^2}$, where (hkl) is the Miller indices, " λ " is the wavelength of incident X-ray (Å), " θ " is the diffraction angle of the peak ($^\circ$)

and "a" is the lattice parameter (Å). The calculated and observed lattice parameters are tabulated in Table 1. Rani R et al (2013) has

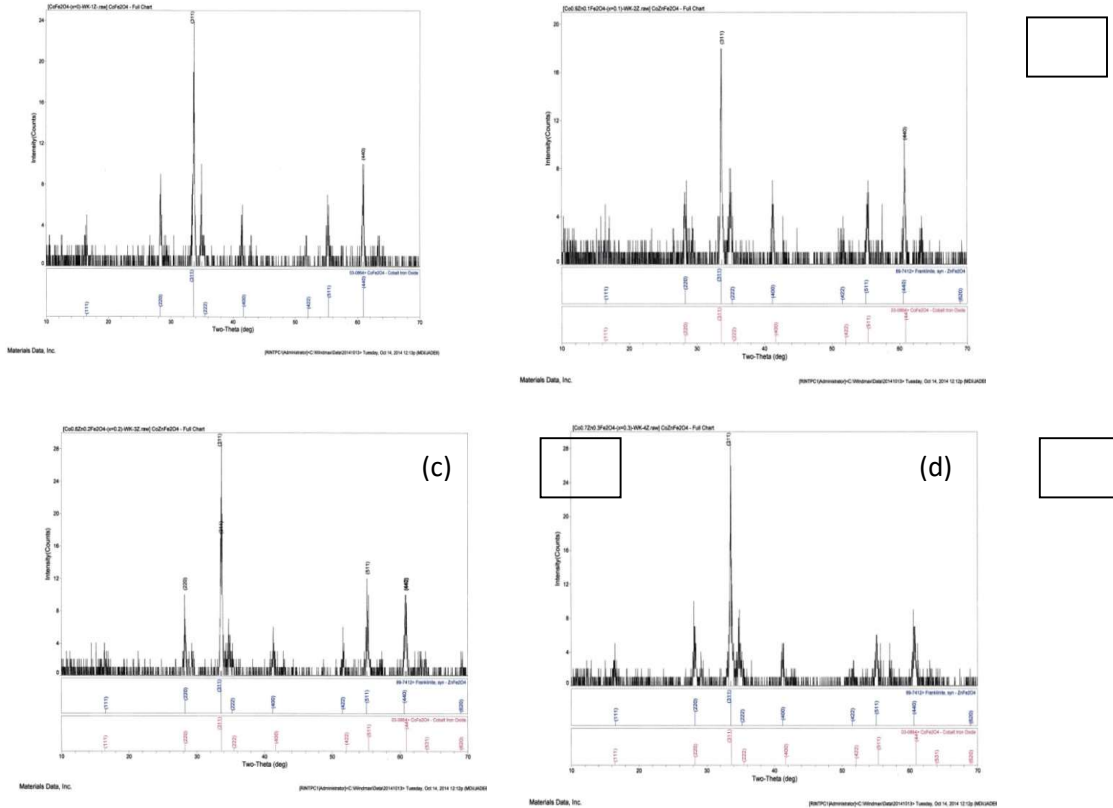


Figure 4. XRD patterns of $\text{Co}_{1-x}\text{Zn}_x\text{Fe}_2\text{O}_4$ where (a) $x = 0.0$, (b) $x = 0.1$, (c) $x = 0.2$ and (d) $x = 0.3$

reported that the $\text{Co}_{1-x}\text{Zn}_x\text{Fe}_2\text{O}_4$ ($x = 0.0, 0.2$ and 0.4) ferrites belong to cubic structure and the lattice parameters are in the range $8.68 \text{ \AA} - 8.91 \text{ \AA}$. In this work, the lattice parameters of the $\text{Co}_{1-x}\text{Zn}_x\text{Fe}_2\text{O}_4$ ($x = 0.0, 0.1, 0.2$ and 0.3) ferrites are obtained as in the range of $8.70 \text{ \AA} - 8.90 \text{ \AA}$ and it almost agreed with that of Rani R et al (2013). Variations of the lattice parameters and crystallite sizes with the concentration of Zn of the samples are shown in Figure 5. The lattice parameters were found to be increased with the increase in concentration of Zn due to the ionic substitution of Zn on Co in the lattice sites.

Crystallite sizes below roughly 100 nm can be evaluated using powder diffraction technique. In this work, the crystallite sizes were estimated by using

the Scherrer formula, $D = \frac{0.9\lambda}{B \cos \theta}$, where "D" is the crystallite size (nm),

"λ" is the wavelength of incident X-ray (Å), "θ" is the diffraction angle of the peak under consideration at FWHM (°) and "B" is the observed FWHM (radians). The obtained average crystallite sizes are also tabulated in Table 1. The obtained average crystallite sizes are nanosized materials.

Table 1. The lattice parameters and crystallite sizes of $\text{Co}_{1-x}\text{Zn}_x\text{Fe}_2\text{O}_4$ (where $x = 0.0, 0.1, 0.2$ and 0.3) ferrites

x	Obs. $a=b=c$ (Å)	Cal. $a=b=c$ (Å)	D (nm)
0.0	8.70	8.70	55.57
0.1	8.71	8.71	41.13
0.2	8.75	8.75	41.97
0.3	8.90	8.90	61.11

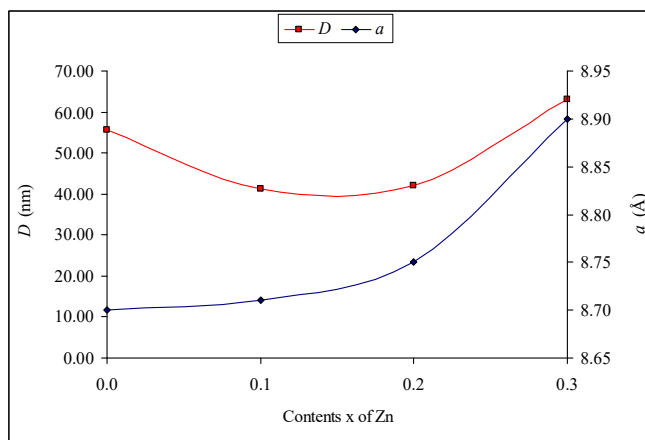


Figure 5. Variations of the lattice parameters and crystallite sizes with increase in Zn concentration of $\text{Co}_{1-x}\text{Zn}_x\text{Fe}_2\text{O}_4$ (where $x = 0.0, 0.1, 0.2$ and 0.3)

Microstructural Analysis

The SEM image is a 2D (2-Dimensional) intensity map in the analog or digital domain. Each image pixel on the display corresponds to a point on the sample, which is proportional to the signal intensity captured by the detector at each specific point. SEM micrograph indicates the microstructural characteristics of the solid materials. SEM micrographs of the samples are shown in Figure 6(a – d) respectively. As shown in figures, the grain shapes of the samples are spherical with poor grain boundary. In all SEM micrographs, some pores are found due to decomposition of starting materials i.e., metal nitrates, water, citric acid and solvent DI water in the sample preparation process. The observed grain sizes of the samples are listed in Table 2. As presented in table, the obtained grain sizes of the samples are different each others. SEM micrographs show that the very fine particles nature.

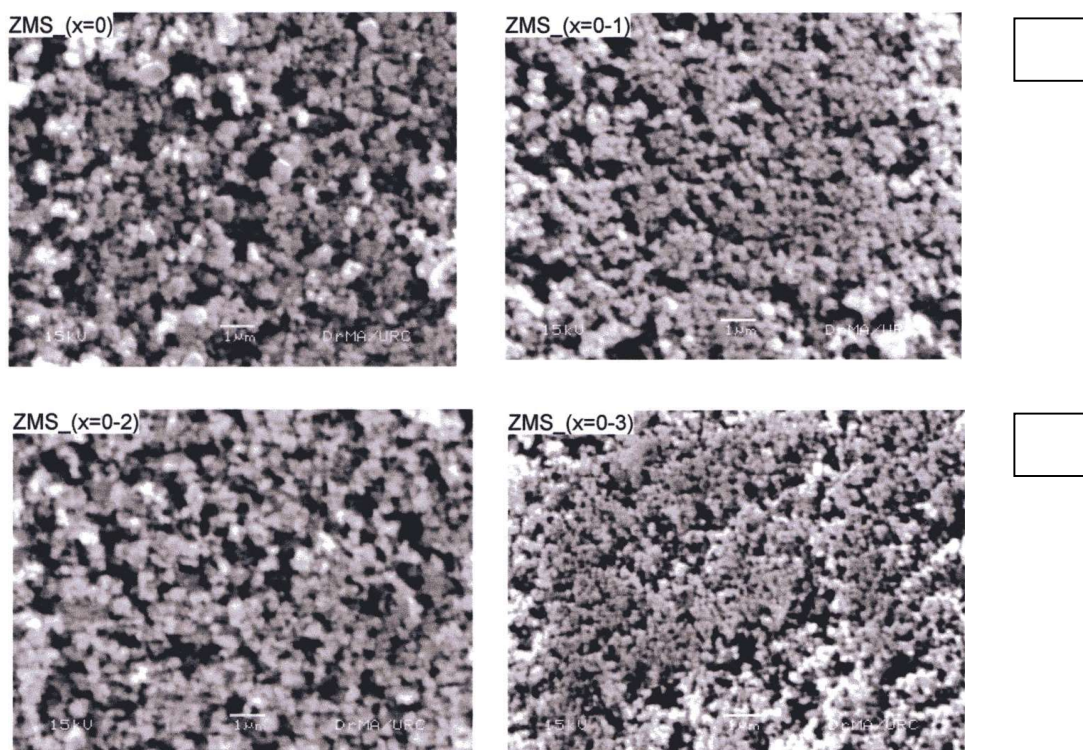


Figure 6. SEM micrographs of $\text{Co}_{1-x}\text{Zn}_x\text{Fe}_2\text{O}_4$ where (a) $x = 0.0$, (b) $x = 0.1$, (c) $x = 0.2$ and (d) $x = 0.3$

Table 2. Grain sizes of $\text{Co}_{1-x}\text{Zn}_x\text{Fe}_2\text{O}_4$ (where $x = 0.0, 0.1, 0.2$ and 0.3) ferrites

x	Grain size (μm)
0.0	0.05 – 0.50
0.1	0.04 – 0.35
0.2	0.06 – 0.50
0.3	0.04 – 0.20

Temperature Dependent Electrical Conductivity Study

The research in the field of Solid-State Ionic encompasses investigations of the physical and chemical behavior of the solids with fast ion movement within the bulk as well as the technological aspects. These materials widely refer to as “Superionic Solids” or “Solid Electrolytes” or “Fast Ion Conductors”, show tremendous scope to develop all solid-state mini/micro electrochemical devices viz. batteries, fuel cells, sensors, etc. The temperature dependent dc electrical conductivity σ of the ferrites obey Arrhenius’s expression: $\sigma = \sigma_0 \exp\left(\frac{-E_a}{kT}\right)$, where, σ_0 is the pre-exponential factor, E_a is activation energy, k is Boltzmann’s constant and T absolute temperature.

Arrhenius’s plots of the dc conductivity of the samples with reciprocal temperature are shown in Figure 7(a – d). The graphs show that the increase in temperature leads to increase in conductivity, which is the normal behaviour of semiconducting materials and it obeys the well known Arrhenius relation. Except the $x = 0.0$ sample, Arrhenius plots of others samples are found to be two portions due to the slope changes in each $\ln \sigma - 1000/T$ curve with the corresponding temperature ranges are shown in Figure 8(a – f). The obtained activation energies of these temperature ranges are listed in Table 3. From the experimental results, the samples exhibited as superionic conductors because their electrical conductivities are greater than 10^{-3} S m^{-1} ($\sigma \geq 1 \times 10^{-3} \text{ Sm}^{-1}$). The superionic phase formation temperatures of the samples are found at 443 K for

$x = 0.0$, 583 K for $x = 0.1$, 753 K for $x = 0.2$ and 643 K for $x = 0.3$ respectively.

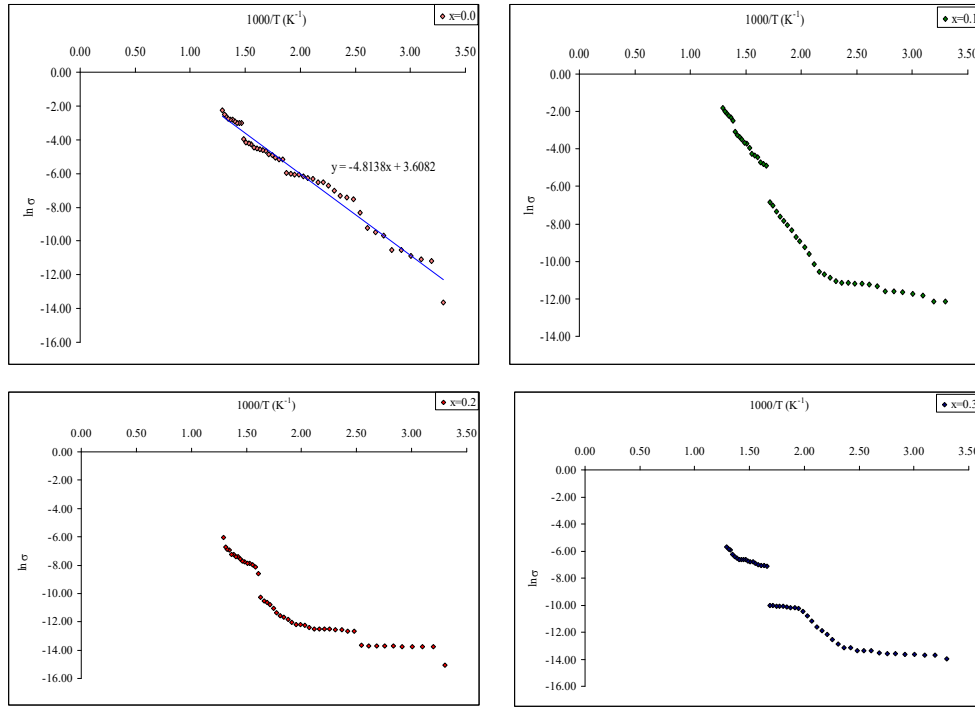


Figure 7. Arrhenius's plots of the dc conductivity with reciprocal temperature of $\text{Co}_{1-x}\text{Zn}_x\text{Fe}_2\text{O}_4$ for (a) $x = 0.0$, (b) $x = 0.1$, (c) $x = 0.2$ and (d) $x = 0.3$

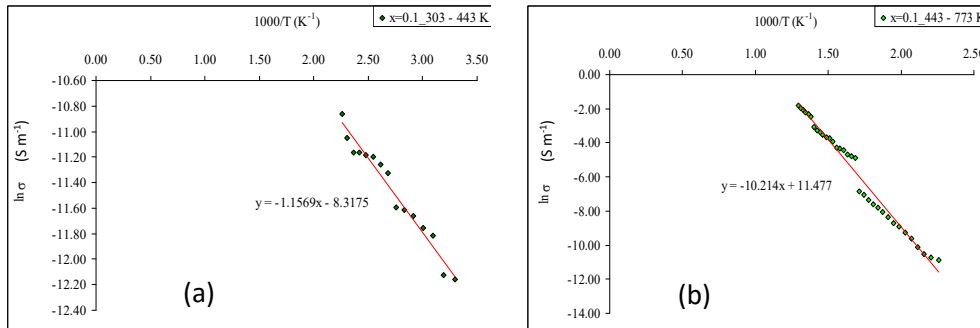


Figure 8. Arrhenius's plots of the temperature dependent electrical conductivities of $\text{Co}_{1-x}\text{Zn}_x\text{Fe}_2\text{O}_4$ (where $x = 0.1$) (a) in 303 K – 443 K and (b) 443 K – 773 K

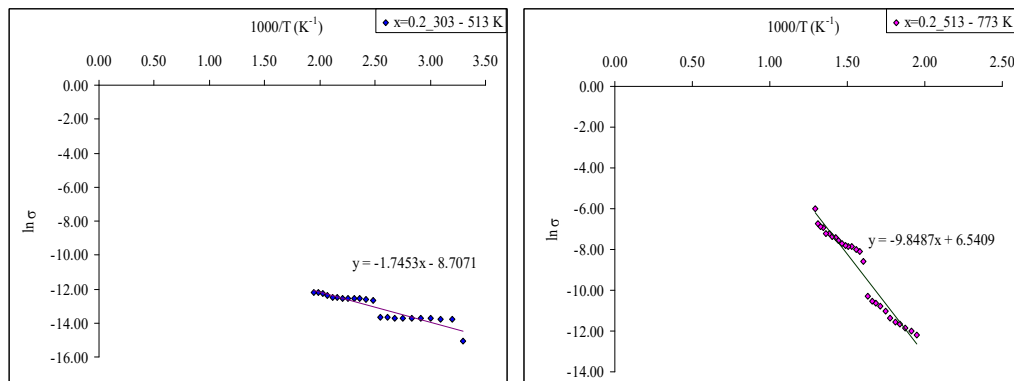


Figure 8. Arrhenius's plots of the temperature dependent electrical conductivities of $Co_{1-x}Zn_xFe_2O_4$ (where $x = 0.2$) (c) in 303 K – 513 K and (d) 513 K – 773 K

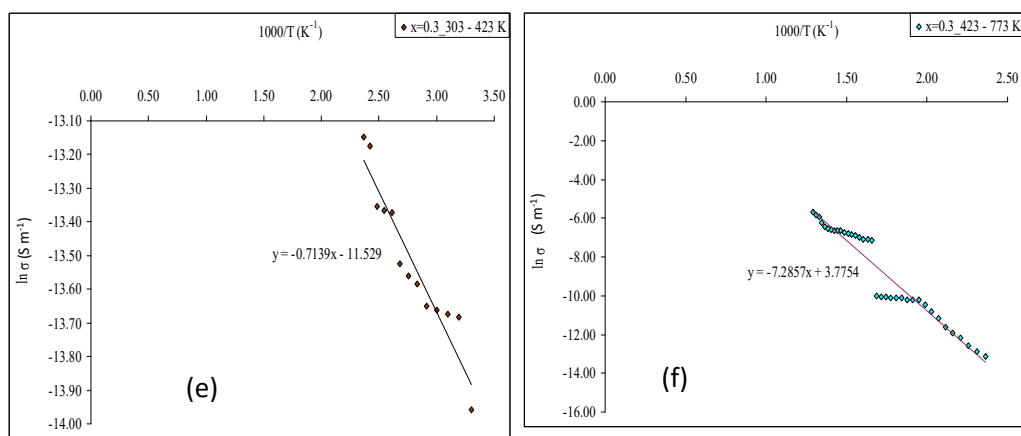


Figure 8. Arrhenius's plots of the temperature dependent electrical conductivities of $Co_{1-x}Zn_xFe_2O_4$ (where $x = 0.3$) (e) in 303 K – 423 K and (f) 423 K – 773 K

Table 3. The activation energies of the $\text{Co}_{1-x}\text{Zn}_x\text{Fe}_2\text{O}_4$ (where $x = 0.0, 0.1, 0.2$ and 0.3)

x	Temperature range (K)	E_a (eV)
0.0	303 - 773	0.42
0.1	303 - 443	0.11
	443 - 773	0.88
0.2	303 - 513	0.15
	513 - 773	0.85
0.3	303 - 423	0.06
	423 - 773	0.63

Conclusion

$\text{Co}_{1-x}\text{Zn}_x\text{Fe}_2\text{O}_4$ (where $x = 0.0, 0.1, 0.2, 0.3$) nanoferrites have been prepared by auto-combustion method. Structural, vibrational and temperature dependent electrical conductivity of the samples were reported in this paper. The X-ray diffraction confirmed the presence of spinel phase cubic crystalline as major phase of the samples. The lattice parameters were found to be increased with the increase in concentration of Zn due to an ionic substitution of Zn^{2+} on Co^{2+} atomic lattice sites. The particle sizes were estimated by using the Scherrer formula and obtained as nanosized ferrite crystallites. SEM micrographs showed that the very fine samples nature. The grain shapes were spherical shapes and they have occurred poor grain boundary. The obtained grain sizes of $\text{Co}_{0.7}\text{Zn}_{0.3}\text{Fe}_2\text{O}_4$ were in the range $0.04 \mu\text{m} - 0.20 \mu\text{m}$ and it was the most homogeneous and the smallest size among the samples. Variation of grain sizes indicated that the grain size depended on Zn concentration. Temperature dependent electrical conductivity results showed that the samples exhibited as the superionic conductors in the high temperatures with the activation energies less than 1 eV. The experimental results can be concluded that the samples can be used as the solid electrolyte materials because they are superionic conductors and their activation energies are obtained as less than 1 eV.

Acknowledgement

The authors would like to acknowledge Professor Dr Khin Khin Win, Head Department of Physics, University of Yangon, for her valuable discussions and comments on this work.

References

1. Ahmad, I. & Farid, M.T. (2012). Characterization of Cobalt Based Spinel Ferrites with Small Substitution of Gadolinium. *World Applied Sciences Journal*, 19, pp. 464-469.
2. Harris, V.G., Geiler, A., Chen, Y., Yoon, S.D., Wu, M., Yang, A., Chen, Z., He, P., Parimi, P.V., Zuo, X., Patton, C.E., Abe, M., Acher O. & Vittoria, C. (2009). Recent advances in processing and applications of microwave ferrites. *Journal of Magnetism and Magnetic Materials*, 321, pp. 2035-2047.
3. Iyer, R., Desai, R. & Upadhyay, R.V. (2009). Low temperature synthesis of nanosized $Mn_{1-x}Zn_xFe_2O_4$ ferrites and their characterizations. *Bulletins Materials Science*, 32, pp. 141-147.
4. Marial, K.H., Choudhury, S. & Hakim, M.A. (2013). Structural phase transformation and hysteresis behavior of Cu-Zn ferrites. *International Nano Letters*, 3, pp. 1-10.
5. Pathan, A.N., Sangshetti, K. & Pangal, A.A.G. (2010). Synthesis and Mossbauer Studies on Nickel-Zinc-Copper Nanoferrites, *Nanotechnology and Nanoscience*, 1(1), pp. 13-16.
6. Rani, R., Kumar, G., Batoor, K.M. & Singh, M.G. (2013). Electric and Dielectric Study of Zinc Substituted Cobalt Nanoferrites Prepared by Solution Combustion Method, *American Journal of Nanomaterials*, 1(1), pp. 9-12.